Cavity-less on-chip optomechanics using excitonic transitions in semiconductor heterostructures

Hajime Okamoto[1], Takayuki Watanabe[1,2], Ryuichi Ohta[1], Koji Onomitsu[1], Hideki Gotoh[1], Tetsuomi Sogawa[1] & Hiroshi Yamaguchi[1,2]

The hybridization of semiconductor optoelectronic devices and nanomechanical resonators provides a new class of optomechanical systems in which mechanical motion can be coupled to light without any optical cavities. Such cavity-less optomechanical systems interconnect photons, phonons and electrons (holes) in a highly integrable platform, opening up the development of functional integrated nanomechanical devices. Here we report on a semiconductor modulation-doped heterostructure–cantilever hybrid system, which realizes efficient cavity-less optomechanical transduction through excitons. The opto-piezoelectric backaction from the bound electron–hole pairs enables us to probe excitonic transition simply with a sub-nanowatt power of light, realizing high-sensitivity optomechanical spectroscopy. Detuning the photon energy from the exciton resonance results in self-feedback cooling and amplification of the thermomechanical motion. This cavity-less on-chip coupling enables highly tunable and addressable control of nanomechanical resonators, allowing high-speed programmable manipulation of nanomechanical devices and sensor arrays.

[1] NTT Basic Research Laboratories, Nippon Telegraph and Telephone Corporation, Atsugi 243-0198, Japan. [2] Department of Physics, Tohoku University, Sendai, Miyagi 980-8578, Japan. Correspondence and requests for materials should be addressed to H.O. (email: okamoto.hajime@lab.ntt.co.jp).

Optical control of nanomechanical resonators has been widely demonstrated in cavity-integrated optomechanical systems[1–12]. In these schemes, photons confined in a cavity cause radiation pressure or photothermal backaction onto a mechanical resonator, which acts in a time delay with respect to the mechanical motion. This leads to self-feedback that can cool and amplify the mechanical motion when the photon energy is red or blue detuned from the cavity resonance[1–3]. Although the cavity optomechanics allows highly tunable control of a single nanomechanical resonator, it cannot be straightforwardly extended to integrated nanomechanical systems, such as nanomechanical circuits and sensor arrays[13–19]. This is because it needs delicate cavity operation, including tapered fibre access, coupling adjustment, cavity stabilization and fine detuning[1–3]. Therefore, alternative approaches are highly demanded in order to practically apply the optical control capability to integrated nanomechanical systems. One approach being developed is based on optomechanical crystals in which photons and phonons are co-localized using band gap[20]. The two-dimensional crystals have been recently realized[21], where the optomechanical arrays would eventually be connected by on-chip waveguides. However, such systems require strong link between structural dimensions and the optical wavelength to spatially collaborate the optical mode with the mechanical mode. Thus, a more scalable 'cavity-less' scheme that also allows free-space optical access is strongly desired to be developed.

Cavity-less optomechanical coupling based on the free-space optical access has recently been demonstrated in several III–V semiconductor micro/nanomechanical systems[22–24]. Yeo et al. and Montinaro et al. have reported the coupling of exciton and mechanical motion in quantum dot-nanowire hybrid systems[22,23]. They were inspired by the theoretical proposal, by Wilson-Rae et al., of sideband cooling using a quantum two-level systems[25]. However, the cooling has not been experimentally implemented because the linewidth of the exciton resonance is orders of magnitude larger than the mechanical resonance frequency, which makes it difficult to achieve efficient optomechanical self-feedback through the phonon-exciton parametric coupling. As a different approach, Okamoto et al. have reported the opto-piezoelectric backaction through electron–hole (e–h) pairs in an n/i-GaAs bilayered cantilever[24]. Spatial separation of electrons and holes due to the built-in electric field causes retarded opto-piezoelectric backaction, which leads to self-feedback on the mechanical resonator. However, the broad absorption edge screens the sharp exciton resonance. This results in inefficient optomechanical self-feedback that prevents the realization of mode cooling.

Here we demonstrate exciton-mediated strong opto-piezo-electric backaction, which allows cavity-less cooling and amplification of a mechanical mode based on the free-space optical access. We use a cantilever with a GaAs/AlGaAs modulation-doped heterostructure, in which photoexcited e–h pairs are bound to form excitons by Coulombic interactions[26]. This structure results in sharply defined exciton resonance (FWHM $\equiv \Delta E_e \simeq 1$ meV and the equivalent quality factor $Q_e \equiv E_e/\Delta E_e = 1,500$), which plays the similar role as an optical cavity. The photon energy detuning from exciton resonance activates the optomechanical self-feedback as in the case of standard cavity optomechanics. It should be noted that the backaction force is not caused by the phonon-exciton parametric coupling[25] but by the carrier-induced piezoelectric force[24] in our sample. Since ΔE_e is five orders of magnitude larger than the mechanical resonance frequency ($f_0 = \omega_0/2\pi = 386.68$ kHz), the parametric coupling is negligibly small. Nevertheless, efficient optomechanical self-feedback is induced via the opto-piezoelectric effect through excitons. This is because the

corresponding time delay ($\tau = 0.4$–0.8 µs), which comes from the spatial confinement of free e–h pairs to form their bound state, is comparable to the mechanical oscillation period. This retarded backaction realizes cooling as well as amplification of the mechanical mode without any optical cavities. Cooling of the fundamental mechanical mode ($Q_m = 5,600$) by a factor of 2 from the bath temperature ($T = 9.2$ K) is achieved with laser irradiation of 3 µW.

Results

Opto-piezoelectric driving. Figure 1a shows an optical micro-graph of the cantilever. The GaAs/AlGaAs modulation-doped heterostructure provides not only a built-in electric field as shown in Fig. 1b, but also sharp excitonic absorption at around 1.515 eV at cryogenic temperatures, which can be confirmed through the intensity I of the photoluminescence excitation (PLE) spectrum (Fig. 2d). These characteristics are necessary in order to obtain the enhanced opto-piezoelectric backaction from bound e–h pairs, namely excitons, via the time-delayed separation of electrons and holes. To generate e–h pairs, we focused a wavelength-tunable Ti:Sa laser on a leg of the U-shaped cantilever where optomechanical coupling is effectively induced via strain (Fig. 2a).

The generation of opto-piezoelectric backaction was confirmed by the following driven measurement: the intensity of the Ti:Sa laser was sinusoidally modulated, while the frequency was swept around the fundamental mechanical mode. The frequency response of the cantilever was measured in a vacuum (5×10^{-5} Pa) by Doppler interferometry with a He:Ne laser (633 nm). This laser was focused near the free-edge of the cantilever where larger displacement results. The frequency response when the photon energy was set to the exciton resonance energy ($E_e = 1.5152$ eV) shows the Lorentzian resonance (Fig. 2b), which displays the optically driven fundamental mechanical mode. The photon-energy dependence of the frequency response reveals that the vibration amplitude is maximized at the exciton resonance energy (Fig. 2c). This indicates the resonator is driven by the opto-piezoelectric process mediated by e–h pairs with the following mechanism[24]: photo-excited electrons and holes in the GaAs layer are separated by the built-in electric field along the thickness direction (Fig. 1b), generating a dipole moment (Fig. 2a). This leads to piezoelectric
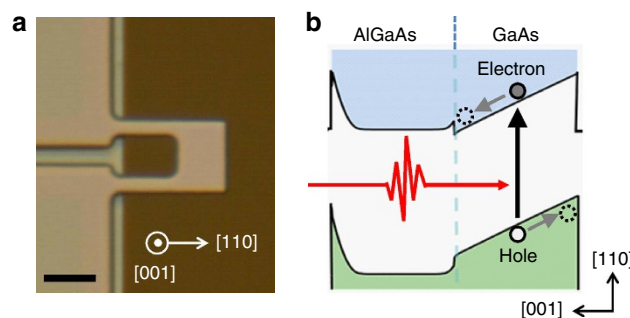

Figure 1 | A semiconductor modulation-doped heterostructure–cantilever hybrid system. (**a**) Optical micrograph of the U-shaped cantilever with a GaAs/AlGaAs modulation-doped heterostructure (scale bar, 10 µm). The fundamental mechanical mode of the [110]-oriented cantilever corresponds to the out-of-plane vibration along [001]. This crystal orientation enables us to utilize opto-piezoelectric backaction in the GaAs-based mechanical system[24,26]. (**b**) Calculated energy-band diagram, in which the separation of photoexcited electrons and holes is schematically drawn. The band-gap energy is about 1.516 eV at cryogenic temperatures.
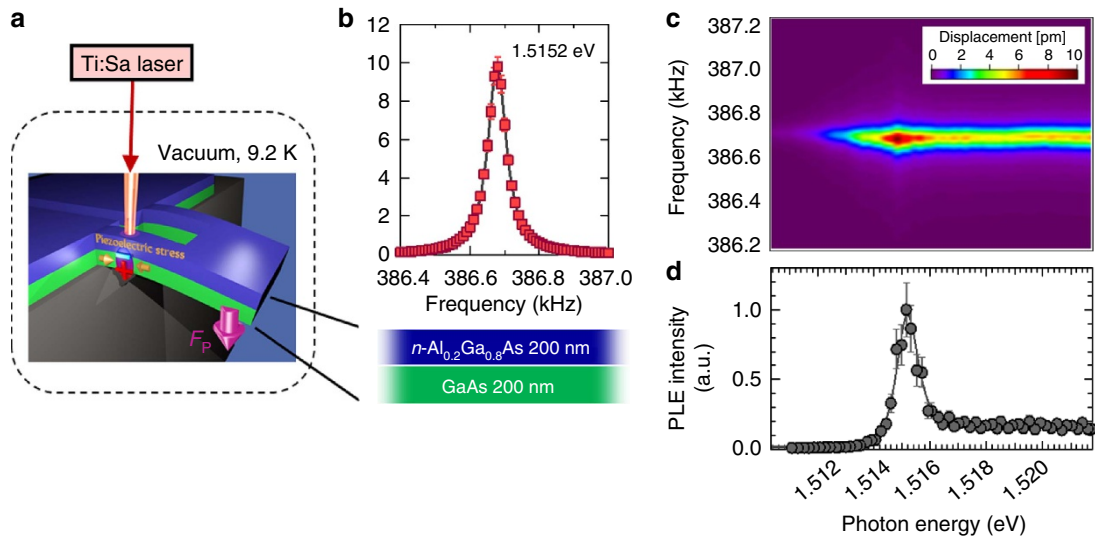
Figure 2 | Optomechanical driving with modulated illumination. (**a**) Schematic drawing of the opto-piezoelectric effect mediated by e–h pairs. Separation of electrons and holes due to the built-in electric field leads to the dipole moment (indicated by a pair of minus and plus), which generates piezoelectric compressive stress (indicated by the yellow arrows). This bends the cantilever as backaction force F_P acts on it (indicated by the purple arrow). (**b**) Frequency response of the cantilever when the photon energy was tuned to the exciton resonance ($E_e = 1.5152$ eV) with the laser power fixed to 0.5 nW. (**c**) Photon-energy dependence of the frequency response under modulated illumination. (**d**) Photoluminescence excitation (PLE) spectrum, which displays a sharp exciton resonance at 1.5152 eV. The error bars are due to the systematic uncertainties in the PLE intensity. The equivalent quality factor of the exciton resonance is $Q_e \equiv E_e/\Delta E_e = 1{,}500$, where ΔE_e is the full width at half maximum of the exciton resonance. a.u., arbitrary unit.

compressive stress, resulting in a bending moment as if the cantilever is subjected to vertical backaction force F_P (Fig. 2a). This backaction force drives the cantilever when it is periodically modulated with the mode frequency by intensity-modulated illumination. The vibration amplitude is sensitive to the photon energy (Fig. 2c) because F_P is proportional to the number of e–h pairs N that contribute the opto-piezoelectric backaction. Thanks to the Q_m-enhanced resonant amplitude, this driven measurement enables a fine mechanical probe of the optical transitions.

Cavity-less cooling and amplification. The opto-piezoelectric backaction results in self-feedback on the thermomechanical vibration when the cantilever is constantly illuminated with the Ti:Sa laser with the slight energy detuning from the exciton resonance. Figure 3a,d show the change in the Brownian displacement noise power spectrum of the cantilever when photon energy is red (1.5145 eV) and blue (1.5160 eV) detuned, respectively (see also the magnified PLE spectrum in Fig. 3b). For the red detuning, increasing laser power P_{ex} increases the vibration amplitude with narrowing the linewidth of the resonance, which corresponds to the damping factor (Fig. 3a). Increasing P_{ex} also increases the area of the noise power spectrum that reflects mode temperature T_{eff}, indicating heating of the mechanical mode. In contrast, for the blue detuning, increasing P_{ex} decreases both the amplitude and area with linewidth widening, indicating cooling of the mechanical mode (Fig. 3d). The photon-energy dependence of normalized mode temperature T_{eff}/T for $P_{ex} = 1.19\,\mu$W clearly shows heating (amplification) in the red-detuning region and cooling in the blue-detuning region (Fig. 3c). This indicates the self-feedback is caused by the strain-induced change in the exciton resonance (Supplementary Note 5), where the feedback efficiency depends on the slope of the absorption (PLE) spectrum.

As shown in Fig. 3e, the exciton resonance is modulated by strain via the deformation potential[27]. Since the excitons sit in the lower half of the cantilever (in the GaAs layer) the exciton

resonance is red shifted when the cantilever bends upwards (purple broken curve in Fig. 3e) and blue shifted when it bends downwards (blue broken curve in Fig. 3e). Therefore, when the photon energy is red detuned, the upward bending increases the dipole moment with an increase in absorption, leading to an increase in the backaction force, that is, $F_P + \delta F_P$ (left top schematic in Fig. 3e). Conversely, the downward bending decreases the dipole moment with a decrease in absorption, leading to a decrease in the backaction force, that is, $F_P - \delta F_P$ (left bottom schematic in Fig. 3e). That is, the backaction force is dependent on strain and the displacement, z. In this red-detuned case, the sign of force gradient ∇F_P ($= \partial F_P/\partial z$) is negative. This negative ∇F_P and the corresponding time delay $\tau \simeq \omega_0^{-1}$ (Supplementary Fig. 1 and Supplementary Note 4) result in the efficient amplification effect around the mechanical resonance frequency $\omega \sim \omega_0$ while reducing the damping factor (see equation (1) in the next paragraph). In contrast, when photon energy is blue detuned, the upward bending decreases the backaction force, that is, $F_P - \delta F_P$ (right top schematic in Fig. 3e), whereas the downward bending increases it, that is, $F_P + \delta F_P$ (right bottom schematic in Fig. 3e). Therefore, ∇F_P is positive in this blue-detuned case and it leads to the efficient damping effect. Note that the above detuning dependence is the opposite of sideband amplification/damping[1,25]. In this excitonic optomechanics, the feedback is caused by strain-induced modulation of the number of e–h pairs. Thus, the polarity of the feedback is determined by the sign of the slope in the absorption (PLE) spectrum and also by the sign of the piezoelectric coefficient[27].

The damping factor modified by this opto-piezoelectric backaction Γ_{eff} can be given by[24]

$$\Gamma_{eff} = \Gamma\left(1 + \frac{Q_m \omega_0 \tau}{1 + \omega^2 \tau^2}\frac{\nabla F_P}{K}\right), \qquad (1)$$

where Γ is the bare damping factor, K is the bare spring constant, and τ is the delay time for the opto-piezoelectric backaction (Supplementary Note 1). Modified mode temperature T_{eff} is
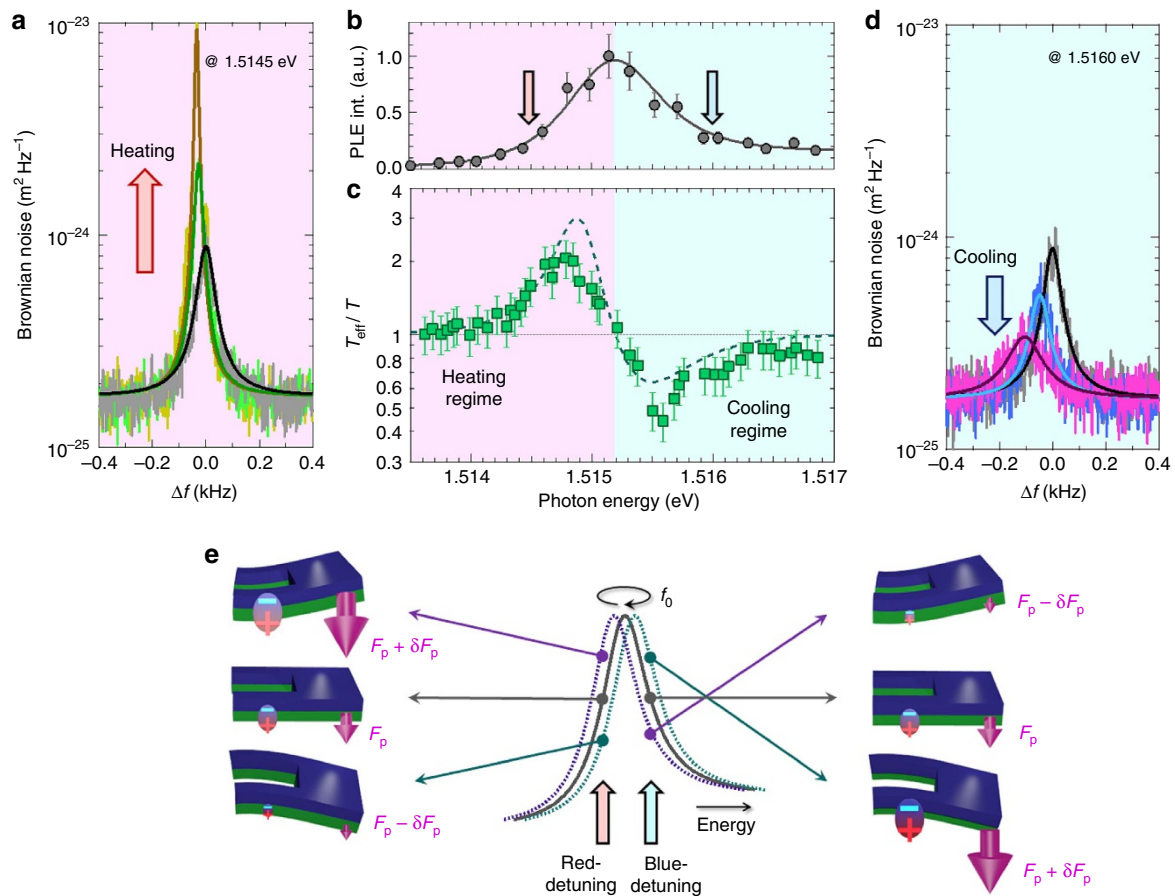
Figure 3 | Amplification (heating) and cooling of the mechanical mode with constant illumination. (a) Brownian displacement noise power spectrum for $P_{ex} = 0$ (black), 1.82 (green) and 2.95 μW (yellow) at 1.5145 eV (red detuning). The solid line is the Lorentzian fit. The horizontal axis show the shift from f_0. **(b)** PLE spectrum in the vicinity of the exciton resonance. The red and blue arrows indicate the detuning point for **a** and **d**, respectively. **(c)** The photon-energy dependence of normalized mode temperature T_{eff}/T for $P_{ex} = 1.19$ μW. The error bars are based on the fitting of the Brownian noise power spectrum to the Lorentzian function. The broken line is a fit with the theoretical form $T_{eff}/T = (1 + C dI/dE)^{-1}$, where dI/dE is the derivative of the PLE intensity I. **(d)** Brownian displacement noise power spectrum for $P_{ex} = 0$ (black), 1.19 (blue) and 5.16 μW (purple) at 1.5160 eV (blue detuning). **(e)** Schematic drawing of the strain-modulated exciton resonance and the strain-dependent opto-piezoelectric backaction for red and blue detuning. A pair of minus and plus indicates the dipole moment induced by the separation of electrons and holes. The purple arrow indicates the strain-dependent opto-piezoelectric backaction force.

inversely proportional to Γ_{eff} as[24]

$$\frac{T_{eff}}{T} = \frac{\Gamma}{\Gamma_{eff}}, \qquad (2)$$

where T is the bath temperature. In the excitation regime of $P_{ex} < 10$ μW, F_p is proportional to P_{ex}, which is confirmed by the vibration amplitude in the driven measurement (Supplementary Fig. 2). This means that the band flattening caused by the screening effect is negligibly small in this power regime; thus, ∇F_p in equation (1) is proportional to P_{ex}. Since the backaction force depends on the strain-induced change in the number of e–h pairs for a fixed laser power, ∇F_p is also proportional to the slope of the PLE spectrum. Therefore, the mode temperature reflects dI/dE, following the theoretical form $T_{eff}/T = \Gamma/\Gamma_{eff} = (1 + C dI/dE)^{-1}$ (broken line in Fig. 3c; Supplementary Note 1), where E is the detuning energy from the excition resonance and C is a coefficient.

Figure 4a shows the laser power dependence of the feedback gain, which corresponds to Γ/Γ_{eff}, when the photon energy is set to 1.5145 (red detuning) and 1.5160 eV (blue detuning). For the red detuning, the gain increases with P_{ex} with the reduction of Γ_{eff}, and for $P_{ex} > 5$ μW, the system enters the self-oscillation (negative damping) regime[9]. In contrast, for the blue detuning, increasing laser power decreases the gain for $P_{ex} < 15$ μW,

following the theoretical form given by equation (1). In the stronger excitation regime ($P_{ex} \geq 15$ μW), on the other hand, an additional effect appears, and it suppresses the damping caused by the opto-piezoelectric backaction in blue detuning. As a result, Γ/Γ_{eff} has a minimum at $P_{ex} = 20$ μW for 1.5160 eV (Fig. 4a). The overall data can be fitted by a modified equation (1), in which the additional backaction force with the opposite sign, $-\nabla F_a$, is also taken into account (blue broken curve in Fig. 4a; Supplementary Note 2), though the origin of this additional effect is not clear at present.

The laser power dependence of T_{eff}/T shows good agreement with that of Γ/Γ_{eff} in the excitation regime of $P_{ex} < 3$ μW (Fig. 4b) as described in equation (2). In contrast, for $P_{ex} \geq 3$ μW, T_{eff}/T deviates from Γ/Γ_{eff} (Fig. 4b). This indicates the existence of another effect that increases the noise temperature as $T \to T + T_b$. We found that T_b has P_{ex}^2 dependence, which appears when optical absorption occurs by band-gap excitation, being irrelevant to the exciton resonance (Supplementary Figs 3–5 and Supplementary Note 3). Modifying equation (2) as $T \to T + T_b$ results in a good agreement between T_{eff}/T and Γ/Γ_{eff} (see the solid line in Fig. 4b). The non-negligible T_b draws back the minimum mode temperature, but a reduction by ~0.5 is still achieved in this system.
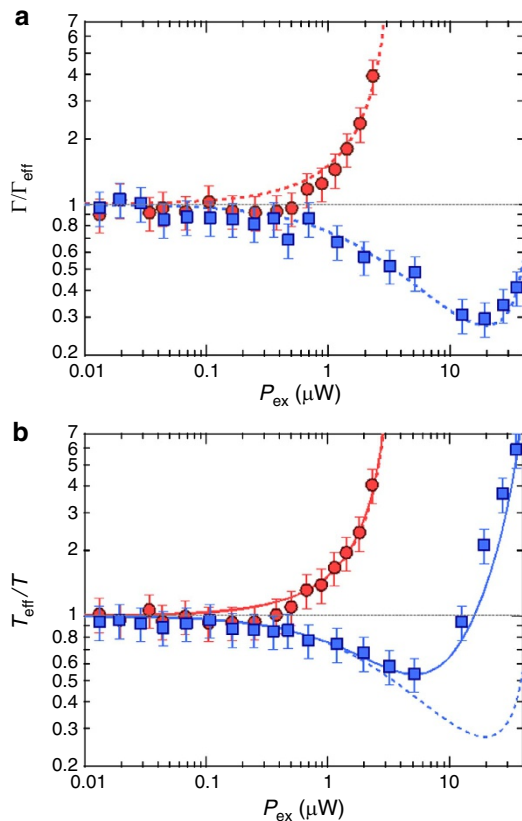
Figure 4 | Comparison of the feedback gain and mode temperature.
(**a**) P_{ex} dependence of feedback gain (Γ/Γ_{eff}) for 1.5145 (red) and 1.5160 eV (blue). The broken line is a fit according to the modified equation (1), in which the opto-piezoelectric backaction (∇F_p) with the linear P_{ex} dependence and the additional backaction force ($-\nabla F_a$) with the $P_{ex}^{1.2}$ dependence are both taken into account. (**b**) Laser power dependence of T_{eff}/T for 1.5145 (red) and 1.5160 eV (blue). The solid line is a fit according to $T_{eff}/(T + T_b) = \Gamma/\Gamma_{eff}$, where $T_b \propto P_{ex}^2$. The broken lines in **b** are identical to those in **a**. The error bars are based on the fitting of the Brownian noise power spectrum to the Lorentzian function.

Discussion

As we have shown in equation (1), the gain of the opto-piezoelectric self-feedback depends on the mechanical quality factor, Q_m. Therefore, the feedback efficiency will be improved in a higher Q_m resonator, which can be prepared, for example, by introducing tensile stress[28]. Hybridizing quantum dots[22,23,29] or quantum wells[30] that cause a sharper optical transition will also improve the coupling efficiency (Supplementary Note 6). Such improved systems open the way to novel optoelectromechanical integrated systems based on a semiconductor device platform. The on-chip hybridization with optical devices, such as like photo detectors and light emitting diodes,[31] further expand the integration capability. This cavity-less coupling enables highly tunable vibration control of nanomechanical resonators via the addressable free-space optical access. This would, therefore, allow high-speed programmable manipulation of integrated nanomechanical systems, which expands their functionality in sensor, signal processing and information technologies[13–19].

Methods

Fabrication. The cantilever (20 μm length and 14 μm width with 10-μm long 4-μm wide legs) was fabricated by photolithography and wet etching. It consists of 200-nm thick Si-doped $Al_{0.2}Ga_{0.8}As$ (including a 5-nm thick GaAs cap layer) and 200-nm thick undoped GaAs, grown on a 3-μm thick $Al_{0.65}Ga_{0.35}As$ sacrificial layer on a GaAs(001) substrate by the molecular beam epitaxy method. To avoid unintentional formation of an optical cavity between the cantilever and substrate, we removed the substrate below the free-standing part by selective cutting.

Measurement. The cantilever was cooled with a cryocooler (ARS: DE-210). The Brownian motion of the cantilever was measured by He:Ne laser interferometry (NeoArk:MLD-221) with a spectrum analyser (HP:89410A). A wavelength-tunable cw Ti:Sa laser (Spectra Physics:3900S) was used for the optical excitation. The He:Ne laser was focused near the free-edge to detect the mechanical motion sensitively, while the Ti:Sa laser was focused on the leg where larger strain is obtained.

References

1. Aspelmeyer, M., Kippenberg, T. J. & Marquardt, F. Cavity optomechanics. *Rev. Mod. Phys.* **86,** 1391–1452 (2014).
2. Marquardt, F. & Girvin, S. M. Trend: optomechanics. *Physics* **2,** 40 (2009).
3. Favero, I. & Karrai, K. Optomechanics of deformable optical cavities. *Nat. Photon.* **3,** 201–205 (2009).
4. Metzger, C. H. & Karrai, K. Cavity cooling of a microlever. *Nature* **432,** 1002–1005 (2004).
5. Arcizet, O., Cohadon, P.-F., Briant, T., Pinard, M. & Heidmann, A. Radiation-pressure cooling and optomechanical instability of a micromirror. *Nature* **444,** 71–74 (2006).
6. Gigan, S. *et al.* Self-cooling of a micro-mirror by radiation pressure. *Nature* **444,** 67–70 (2006).
7. Schliesser, A., Riviere, R., Anetsberger, G., Arcizet, O. & Kippenberg, T. J. Resolved-sideband cooling of a micromechanical oscillator. *Nat. Phys.* **4,** 415–419 (2008).
8. Kippenberg, T. J. & Vahala, K. J. Cavity optomechanics: back-action at the mesoscale. *Science* **321,** 1172–1176 (2008).
9. Metzger, C., Favero, I., Ortlieb, A. & Karrai, K. Optical self cooling of a deformable Fabry-Perot cavity in the classical limit. *Phys. Rev. B* **78,** 035309 (2008).
10. Usami, K. *et al.* Optical cavity cooling of mechanical modes of a semiconductor nanomembrane. *Nat. Phys.* **8,** 168–172 (2012).
11. Chan, J. *et al.* Laser cooling of a nanomechanical oscillator into its quantum ground state. *Nature* **478,** 89–92 (2011).
12. Verhagen, E., Deléglise, S., Weis, S., Schliesser, A. & Kippenberg, T. J. Quantum-coherent coupling of a mechanical oscillator to an optical cavity mode. *Nature* **482,** 63–67 (2012).
13. Habraken, S. J. M., Stannigel, K., Lukin, M. D., Zoller, P. & Rabl, P. Continuous mode cooling and phonon routers for phononic quantum networks. *New J. Phys.* **14,** 115004 (2012).
14. Schmidt, M., Ludwig, M. & Marquardt, F. Optomechanical circuits for nanomechanical continuous variable quantum state processing. *New J. Phys.* **14,** 125005 (2012).
15. Massel, F. *et al.* Multimode circuit optomechanics near the quantum limit. *Nat. Commun.* **3,** 987 (2012).
16. Truitt, P. A., Hertzberg, J. B., Huang, C. C., Ekinci, K. L. & Schwab, K. C. Efficient and sensitive capacitive readout of nanomechanical resonator arrays. *Nano Lett.* **7,** 120–126 (2007).
17. Fritz, J. *et al.* Translating biomolecular recognition into nanomechanics. *Science* **288,** 316–318 (2000).
18. Bargatin, I. *et al.* Large-scale integration of nanoelectromechanical systems for gas sensing applications. *Nano Lett.* **12,** 1269–1274 (2012).
19. Arlett, J. L., Myers, E. B. & Roukes, M. L. Comparative advantages of mechanical biosensors. *Nat. Nanotech.* **6,** 203–215 (2011).
20. Eichenfield, M., Chan, J., Camacho, R. M., Vahala, K. J. & Painter, O. Optomechanical crystals. *Nature* **462,** 78–82 (2009).
21. Safavi-Naeini, A. H. *et al.* Two-dimensional phononic-photonic band gap optomechanical crystal cavity. *Phys. Rev. Lett.* **112,** 153603 (2014).
22. Yeo, I. *et al.* Strain-mediated coupling in a quantum dot-mechanical oscillator hybrid system. *Nat. Nanotech.* **9,** 106–110 (2014).
23. Montinaro, M. *et al.* Quantum dot opto-mechanics in a fully self-assembled nanowire. *Nano Lett.* **14,** 4454–4460 (2014).
24. Okamoto, H. *et al.* Vibration amplification, damping and self-oscillations in micromechanical resonators induced by optomechanical coupling through carrier excitation. *Phys. Rev. Lett.* **106,** 036801 (2011).
25. Wilson-Rae, I., Zoller, P. & Imamoğlu, A. Laser cooling of a nanomechanical resonator mode to its quantum ground state. *Phys. Rev. Lett.* **92,** 075507 (2004).
26. Watanabe, T. *et al.* Optomechanical photoabsorption spectroscopy of exciton states in GaAs. *Appl. Phys. Lett.* **101,** 082107 (2012).
27. Adachi, S. *Properties of Group-IV, III-V and II-VI Semiconductors* (Wiley, 2005).
28. Yamaguchi, H. *et al.* Improved resonance characteristics of GaAs beam resonators by epitaxially induced strain. *Appl. Phys. Lett.* **92,** 251913 (2008).
29. Marzin, J.-Y., Gérard, J.-M., Izraël, A. & Bastard, G. Photoluminescence of single InAs quantum dots obtained by self-organized growth on GaAs. *Phys. Rev. Lett.* **73,** 716–719 (1994).

30. Gammon, D., Snow, E. S., Shanabrook, B. V., Katzer, D. S. & Park, D. Fine structure splitting in the optical spectra of single GaAs quantum dots. *Phys. Rev. Lett.* **76,** 3005–3008 (1996).

31. Ukita, H., Uenishi, Y. & Tanaka, H. A photomicrodynamic system with a mechanical resonator monolithically integrated with laser diodes on gallium arsenide. *Science* **260,** 786–789 (1993).

Acknowledgements

Author contributions

H.O. and T.W. designed the sample. K.O. grew the heterostructure. T.W. fabricated the cantilever. H.G. performed the PLE measurement. T.W. and R.O. performed the opto-mechanical measurements. H.O. and R.O. analysed the data. H.O. wrote the paper based on the discussion with all the authors. H.Y. planned the project.

Additional information